ADMITTANCE AND CORRELATION OF LOCALIZED GRAVITY AND TOPOGRAPHY OF FREUNDLICH-SHARONOV BASIN OF THE MOON. Noriyuki Namiki, Planetary Exploration Research Center, Chiba Institute of Technology (2-17-1 Tsudanuma, Narashino, Chiba, Japan 275-0016).

Introduction: In 1966, the Luna 10 mission opened a study of the gravity field of the Moon. Continued observations led Muller and Sjogren [1] to discover large positive gravity anomalies called "mascons" over basins covered by mare basalts on the near side. Mascons are important for the study of the internal structure and the evolution of the Moon [2, 3]. However, because all the nearside impact basins are filled with extensive mare basalt deposits, it is difficult to estimate the subsurface structures, such as uplift of the Moho surface, from gravity field model. In contrast, farside impact basins have much less, or often even none, mare basalt coverage. This allows us to investigate the internal structure underneath impact basins, helping to understand dynamics of large impacts and the thermal state of the Moon during the late heavy bombardment period [4].

A new spherical harmonic model of the lunar gravity field, complete to degree and order 100 (SGM100g), has been developed from four-way Doppler measurements of Kaguya [4, 5]. On near side, a comparison of SGM100g with a previous lunar gravity models reveals a general agreement. The five principal gravity highs on Imbrium, Serenitatis, Crisium, Nectaris, and Humorum are clearly visible, as in the previous models. On far side, in contrast, the new gravity field model shows several circular signatures that correspond to topographic structures such as Moscoviense, Freundlich-Sharonov, Mendeleev, Hertzsprung, Korolev and Apollo basins that used to be identified as linear signatures in previous models [4, 5]. New data sets obtained by Kaguya mission have been open to public since November, 2009 [6].

Freundlich-Sharonov basin is classified as Type II basin indicating rigid support of topographic depression of the basin by thick lithosphere, mantle uplift beneath the center of the basin, and partial compensation of the central part [4]. This basin has two ring structures (Figure 1). Similarly with other Type II basins, the topography of this basin is characterized by two floors at different levels. Namely, the floor inside of the inner ring is lower in altitude than the floor between outer and inner rings (Figure 1). This characteristic of Type II basin is markedly different from flat floor of nearside primary mascon basins and elevated floor of Type I basins.

Data Sets and Localization Method: We adopt lunar gravity field and topography models of Kaguya (SGM100g and STM359, respectively) as global data sets [4, 5, 6, 7]. For the spectral analysis of the gravity field of the Moon, it is very important to localize gravity anomalies over a region of interest. During one-year nominal mission of Kaguya, four-way Doppler measurements via relay sub-satellite have completed coverage of far side of the Moon [5]. However, distribution of the four-way Doppler measurements is not uniform because the relay sub-satellite has no propulsion mechanism to control its orbit. Consequently, spherical harmonic coefficients of degree higher than 70 are subject to ill effect of small gaps of data coverage in the northern hemisphere [4, 7]. In addition, strong positive gravity anomalies over mascon basins on near side have a considerable influence on the global spectra at long wavelengths.

For the study of lunar basins of which diameter are comparable to lunar radius, localization by two-dimensional Fourier analysis is not appropriate. Instead, we use spectral filter of wavelet analysis that automatically adjusts a band width so as to remove undesired signals at wavelength longer than the size of studied area properly from local spectra [8]. Then we adopt the method developed by Simons *et al.* [9]. This method also has an advantage to Fourier analysis that the gravity and topography models can be calculated without a loss of spectral information. This advantage is particularly important for distinguishing several compensation mechanisms of the lunar basins.

The mathematical procedures of localization of gravity and topography are described in detail by Simons *et al*. [9, 10, 11] and Wieczorek and Simons [12]. The latter proposed new kinds of windows that maximize spatial energy within a polar cap and spectral power within a spherical harmonic bandwidth to remove bias of stochastic processes from global data optimally. For numerical simplicity, however, we follow the former method and use truncated spherical harmonic expansions of boxcar caps as a window function.

Results: Localized gravity and topography of the Freundlich-Sharonov basin is shown in Figure 2 by solid red and blue lines, respectively. In general, farside basins have rougher surface than nearside mascon basins. Therefore we evaluate local variations in the localized gravity and topography at first by deriving axisymmetric components in the manner of least square fitting. The results are also shown in Figure 2 by dashed lines. It is obvious that the localized gravity and topography of the Freundlich-Sharonov basin are

dominated by axisymmetric components. Thus the basin structure can be adequately modeled by a combination of axisymmetric topography and subsurface mass anomalies.

The localized topography shows two peaks at degree of 20 and 50 in Figure 2. These peaks correspond to two ring structures and respective floors (Figure 1). Because the basin is mostly negative in topography, Stokes coefficients of axisymmetric components are negative, too, for degree greater than 4. In contrast, the localized gravity field shows two peaks at degree of 19 and 35. At degree of 19, Stokes coefficients of axisymmetric gravity are negative, while the coefficients are positive at degree of 35.

Evidently the peaks of the localized gravity and topography at degrees 19 and 20 are related with each other. This inference is confirmed by little variation of Bouguer gravity anomalies at this wavelength (Figure 1). The second peaks, on the other hand, show opposite signs and different peak degrees. Nonetheless, an agreement of central locations of the gravity and topography in Figure 1 strongly suggests relationship between these second peaks as well. The signs of the second peaks probably indicate partial isostatic compensation of positive mass anomalies in the subsurface at the center of the Freundlich-Sharonov basin. And longer peak wavelength of the gravity than topography possibly constrains the depth of the mass anomalies.

Admittance and correlation of the localized gravity and topography are shown in Figure 3 by solid blue and dashed red lines, respectively. Simply speaking, calculated correlations are either 1 or -1. This behavior can be explained by dominance of axisymmetric components. If the pole of the spherical coordinate is set at the center of the Freundlich-Sharonov basin, both localized gravity and topography are essentially expressed by one zonal coefficient for every degree. Thus correlations for any degree would be naturally either 1 or -1. Signs switch as those of axisymmetric components of the localized gravity switches.

References: [1] Muller P. M. and Sjogren W. L. (1968) *Science*, *161*, 680. [2] Solomon S. C. (1984) in *Origin of the Moon*, 435. [3] Watts A. B. (2001) *Isostasy and Flexure of the Lithosphere*, Cambridge Univ. Press. [4] Namiki N. et al. (2009) *Science*, *323*, 900-905. [5] Matsumoto K. et al. (2009) *submitted to JGR*. [6] https://www.soac.selene.isas.jaxa.jp/archive/index.html.en. [7] Araki H. *et al*. (2009) *Science*, *323*, 897-900. [8] Chui, (1992), *An Introduction to Wavelets*, Academic Press. [9] Simons M. *et al.* (1997) *GJI*, *131*, 24-44. [10] Simons M. *et al.* (1994) *Science*, *256*, 798-803. [11] Simons M. (1995) *PhD thesis*, MIT. [12] Wieczorek M. A. and Simons F. J. (2005) *GJI*, *162*, 655-675.

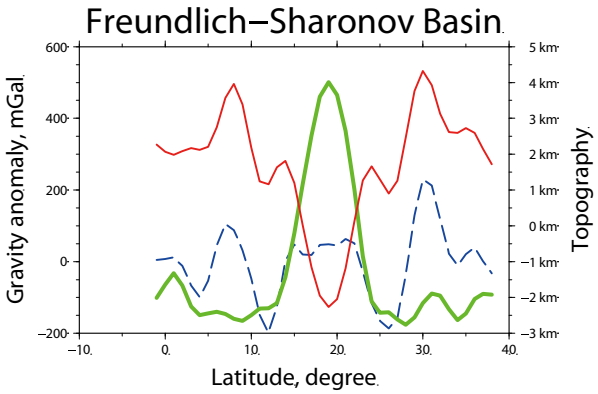

Figure 1. Longitudinal cross sections of global free-air gravity anomalies (dashed blue line), Bouguer gravity anomalies (thick green line), and topography (thin red line) of the Freundlich-Sharonov basin. Local variations are removed by averaging four neighboring cross sections.

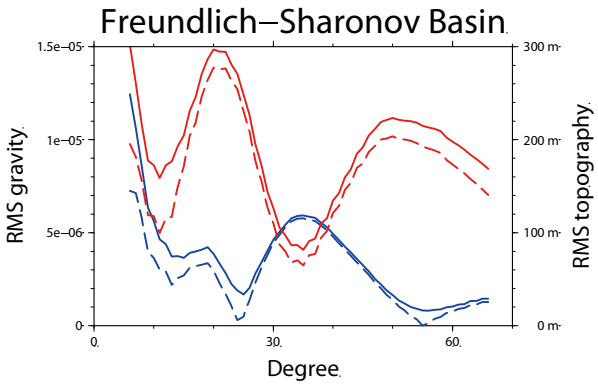

Figure 2. Root mean square of localized gravity (blue solid line) and topography (red solid line) of the Freundlich-Sharonov basin. Dashed lines are axisymmetric components of the gravity (blue line) and topography (red line) fields, respectively.

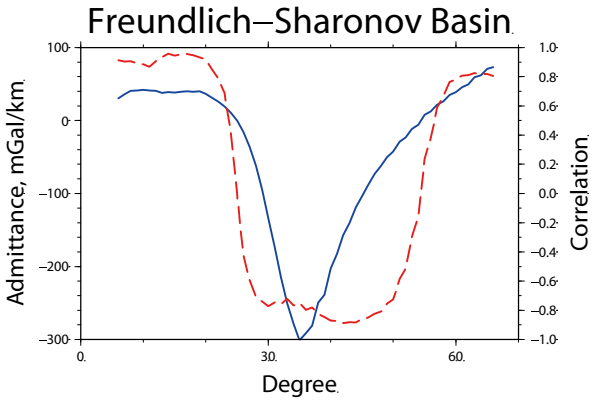

Figure 3. Admittance (blue line) and correlation (red line) of the localized gravity and topography of the Freundlich-Sharonov basin.